

06.1

## Synthesis of Au/Si nanostructures by STM lithography

© D.V. Lebedev<sup>1–3</sup>, V.A. Shkoldin<sup>1,4</sup>, A.M. Mozharov<sup>2</sup>, A.E. Petukhov<sup>2</sup>, A.O. Golubok<sup>3</sup>, A.V. Arkhipov<sup>5</sup>,  
I.S. Mukhin<sup>1,5</sup>, V.G. Dubrovsky<sup>2</sup>

<sup>1</sup> Alferov Federal State Budgetary Institution of Higher Education and Science Saint Petersburg National Research Academic University of the Russian Academy of Sciences, St. Petersburg, Russia

<sup>2</sup> St. Petersburg State University, St. Petersburg, Russia

<sup>3</sup> Institute of Analytical Instrument Making, Russian Academy of Sciences, St. Petersburg, Russia

<sup>4</sup> ITMO University, St. Petersburg, Russia

<sup>5</sup> Peter the Great Saint-Petersburg Polytechnic University, St. Petersburg, Russia

E-mail: Denis.v.lebedev@gmail.com

Received April 15, 2022

Revised April 26, 2022

Accepted April 29, 2022

A technique for synthesizing nanostructures by current lithography in a scanning tunneling microscope (STM lithography) in layered Au/Si structures has been developed. An experimental dependence of the geometric dimensions of the created nanostructures on the time of current STM lithography has been obtained. A theoretical model for the growth of nanostructures is proposed, which explains the nonlinear dependence of the radius of the obtained nanostructures on time with saturation in the region of large radii.

**Keywords:** Au/Si nanostructures, STM lithography, growth rate, modeling.

DOI: 10.21883/TPL.2022.06.53790.19224

One of the most topical issues in the field of computer engineering development is enhancing the efficiency of the state-of-the-art integrated microchips. A promising approach to solving this problem may be the integration of photonic and electronic components into the new-generation optoelectronic microchips. The photonic components may be conditionally subdivided into three types: sources of optical signals [1], devices for information processing [2,3], and devices for information transmission [4]. Packaged electrically driven sources of optical emission are among the key components of any optoelectronic system. The existing lasers ensuring the solution of this-field problems, such as vertical-cavity lasers [5], microring/microdisk lasers [6] or single-nanoparticle lasers [7], have cavities with geometric sizes significantly exceeding the emission wavelength, which prevents applying them in the integrated optoelectronic systems. Moreover, they are hardly compatible with CMOS technologies. The mentioned drawbacks may be eliminated by replacing local light sources with structures based on the effect of photon emission during inelastic electron tunneling through the nanocontact [8].

Because of its simplicity and universality, the scanning tunneling microscope (STM) is an efficient tool for studying the emission from the tunneling nanocontact [9]. One more STM advantage is the possibility of the surface modification under the probe tip (the STM lithography technique [10,11]). STM allows not only manipulation of sole atoms but also modification of the surface in the specified sample area by passing high-density current [12,13]. There exist several methods for modifying the surface under the STM probe tip, for instance, sublimation or chemical

reaction induced by tunneling electrons, Joule heating, field evaporation, etc. [14].

This paper proposes a new technique for synthesizing nanoscale electrically driven sources of optical emission based on CMOS-compatible materials: Au and Si. For this purpose, STM lithography is used, which enables local modification of the Au/Si thin film stacks by local heating.

To create samples with Au/Si thin films, first the as-cleaved plates of mica  $K_2O \cdot Al_2O_3 \cdot SiO_2$  (TipNano Co, Estonia) were placed into the chamber of the vacuum thermal evaporation setup (Boc Edwards Auto 500, Great Britain). Then the vacuum system was evacuated to the residual pressure no worse than  $10^{-7}$  mbar with subsequent degassing the samples for 15 min at 200°C. After that, Au layers 100 nm thick were applied on the substrates heated to 130°C with the deposition rate of 6–7 nm/min. After the Au deposition, the samples were transferred to the ultrahigh-vacuum chamber of STM Omicron VT AFM XA 50/500 (Scienta Omicron, Germany) where they were additionally annealed at the temperature higher than 150°C in order to remove the adsorbate from the surface. The STM vacuum chamber contained also a module for the Si film thermal deposition. In addition, a layer of undoped Si 10 nm thick was deposited on the Au surface.

The studies employed commercially available Pt/Ir probes DPT10 (Bruker, USA). The STM technique for synthesizing nanostructures on film surfaces consists of several stages illustrated in Fig. 1, *a*. First it is necessary to obtain the topography of the area selected for modification (Fig. 1, *b*) in the mode of low current ( $I_{sp} = 0.1$  nA) at low nanocontact bias voltage ( $V_{bias} = 0.5$  V). Then the probe is displaced to

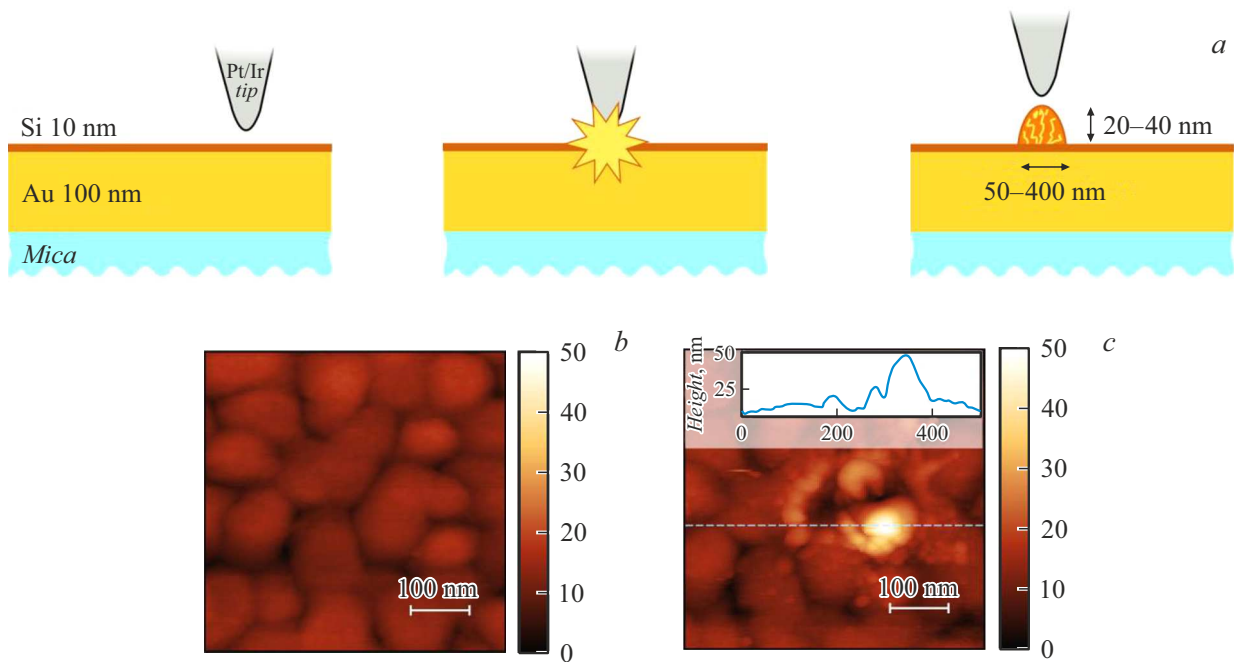


**Figure 1.** *a* — schematic diagram of the technique for creating a composite nanostructure; *b, c* — STM images of the sample surface and created Au/Si nanostructure, respectively. The inset presents the nano-hillock profile.

the selected area, and local modification of the surface is performed by applying an electric pulse  $-10\text{ V}$  in voltage and tens of milliseconds to tens of seconds in length. During the pulse exposure, the STM feedback gets broken. After that, the topography is scanned and visualization of the surface modification results, namely, formation of a nanostructure in the form of a „nano-hillock“ (Fig. 1, *c*), is performed.

It is possible to assume that the mechanism of nano-hillocks formation in layered Au/Si films is connected with local Joule heating by high-density current in the zone beneath the STM probe. Mutual diffusion of the materials in this zone results in formation of the Au/Si composite structure. The STM impact with the same parameters on the Au film does not cause similar surface modifications, which may be explained by that heat transfer in the Au film is more efficient.

The STM image presented in Fig. 1, *c* clearly exhibits coagulated nanometer-diameter droplets around the nano-hillock, which are typical of the thin film local heating. A similar effect may be observed for particles created by laser ablation. Paper [15] describes the formation of hybrid Si/Au nanoparticles from the Si (60 nm)/Au (15 nm) film by laser ablation with a femtosecond laser. As shown in [15], investigation with a transmission electron microscope revealed that those nanoparticles have polycrystalline silicon structure with Au inclusions. We assume that nano-hillocks obtained by STM lithography have a similar composite composition, which opens an opportunity to use such systems as nanoscale sources of optical emission.

To determine the dependence of sizes of the formed nanostructures on parameters of the STM lithography on the sample consisting of a stack of Au (100 nm)/Si (10 nm) films, a set of nano-hillocks fabricated under different conditions was prepared. It was revealed experimentally that the nano-hillock diameter increases with increasing pulse length and current. The nanostructure radius dependence on the pulse length (or exposition time) is of the pronounced nonlinear character (Fig. 2, *a*). The proposed technique ensures formation on the Au/Si thin film surfaces of nanostructures with the minimal radius of about 30 nm.

To explain the nonlinearity of the nanostructure radius dependence on the exposition time (see Fig. 2, *a*), let us use the relation for the rate of the particle number increase in nucleus  $i$  [16–18] which is conventional for the nanostructure growth theory:

$$\frac{di}{dt} = \frac{\xi(t)}{\tau} i^p. \quad (1)$$

Here  $\xi(t)$  is the oversaturation (excess concentration) caused by local heating of the Au/Si film during STM lithography,  $\tau$  is the characteristic growth time,  $p$  is the power index varying in the  $0 \leq p < 1$  range (typically,  $p = 0, 1/3, 1/2, 2/3$ , depending on the mass transfer mechanism [16,17]). It is reasonable to assume that the oversaturation decreases from a certain maximum  $\xi_0$  to zero because of the temperature equalization and vanishing of local heating due to the thermal conductivity. We use for  $\xi(t)$  the power-law model  $\xi(t) = \xi_0 / (1 + t/t_*)^\alpha$ , where  $t_*$  is the characteristic time of the oversaturation reduction,  $\alpha > 0$  is the power index. To our opinion, the nano-hillock

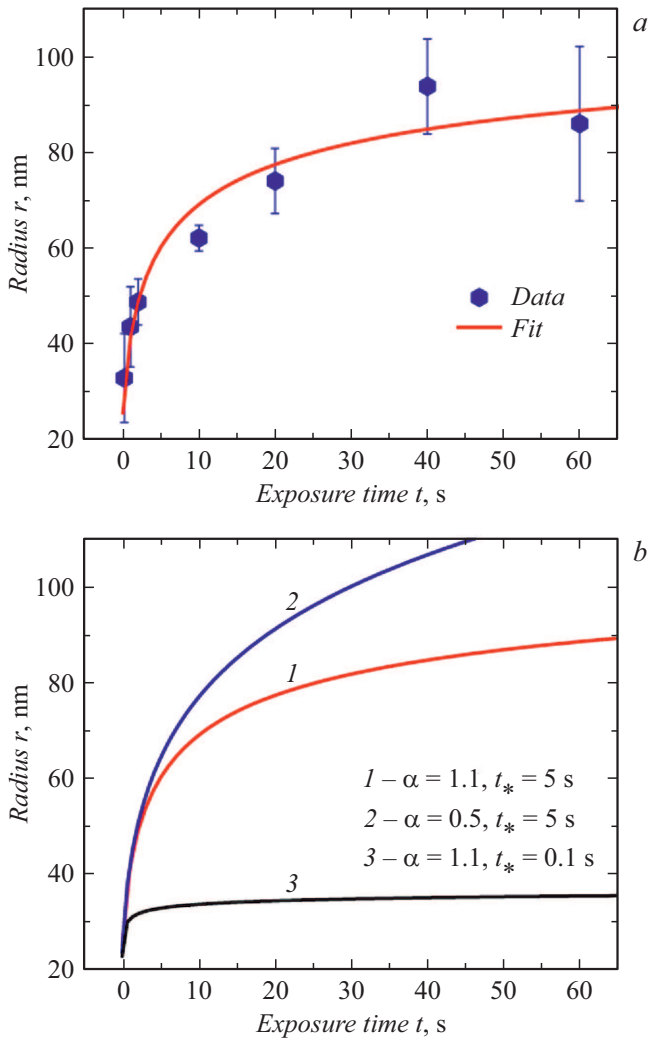


**Figure 2.** *a* — the nano-hillock radius versus the time of exposure, in the framework of STM lithography, to different-length pulses with equal preset currents (20 nA) and bias voltages (−10 V). Symbols represent the measured dependence; the curve was obtained via relation (2) at  $r_0 = 25$  nm,  $A = 60\,000$ ,  $t_* = 5$  s,  $\alpha = 1.1$  and  $p = 0$ . *b* — theoretical time dependence of radius at different parameters. Curve 1 is the same as in panel *a*, curve 2 corresponds to the unlimited growth at  $\alpha = 0.5$ , curve 3 corresponds to the growth suppression at low  $t_* = 0.1$  s due to fast reduction of oversaturation.

shape is defined by the surface energy state and persists during the growth [19]; thus, the relationship between  $i$  and radius  $r$  may be expressed as  $i = Cr^3$ , where  $C$  is independent of exposition time  $t$ .

Integrating equation (1), obtain for the nanostructure radius

$$r = \left\{ r_0^q + \frac{At_*}{1-\alpha} \left[ \left( 1 + \frac{t}{t_*} \right)^{1-\alpha} - 1 \right] \right\}^{1/q}, \quad (2)$$

where  $q = 3(1-p)$  and  $A = (1-p)\xi_0/(C^{1-p}\tau)$ . The obtained expression provides two important conclusions.

First, the nanostructure radius increases unlimitedly at  $\alpha < 1$ , while at  $\alpha > 1$  this increase is restricted, i.e. the nanostructure radius tends to a constant. Value  $\alpha = 1$  corresponds to the logarithmic growth of radius with time. Second, the nano-hillock formation is possible only when the oversaturation reduction time  $t_*$  is sufficiently large, i.e., the heat transfer should not be too fast. At  $t/t_* \ll 1$ , relation (2) appears as follows:

$$r = (r_0^q + At)^{1/q}, \quad (3)$$

which corresponds to the island growth at constant oversaturation  $\xi_0$  and coincides with the result of [16].

The curve presented in Fig. 2, *a*, which provides the best agreement with experimental data, was obtained from relation (2) at  $A = 60\,000$ ,  $t_* = 5$  s,  $\alpha = 1.1$  and  $p = 0$ . Value  $p = 0$  corresponds to the diffusion-controlled growth of a three-dimensional island at the atom diffusion lengths significantly exceeding the island linear dimensions [17]. Fig. 2, *b* presents the curves corresponding to the unlimited growth at  $\alpha = 0.5$  and almost total absence of the growth at  $t_* = 0.1$  s. The latter qualitatively corresponds to the case of a pure Au film where islands fail to arise because of a more efficient heat removal in the film area under the STM tip due to a higher thermal conductivity of Au as compared with Si.

Thus, the paper presents the technique for the STM-lithography synthesis of nanostructures in layered Au/Si structures. An experimental dependence of the geometric dimensions of the created nanostructures on the time of the current STM lithography has been obtained. A theoretical model explaining the nonlinear character of the nanostructure size dependence on the pulse length has been proposed. This technique was successfully applied to the Au/Si films, which makes it potentially compatible with the up-to-date CMOS procedure.

### Acknowledgements

The studies were performed by using the equipment of Educational Resource Center of SPbSU Scientific Park „Physical methods for surface investigation“.

### Financial support

The study was supported by the Russian Scientific Foundation (project № 21-79-10346). The modeling was supported by the SPbSU grant No 75746688.

### Conflict of interests

The authors declare that they have no conflict of interests.

### References

- [1] J. Kern, R. Kulloock, J. Prangmsma, M. Emmerling, M. Kamp, B. Hecht, *Nature Photon.*, **9**, 582 (2015). DOI: 10.1038/nphoton.2015.141

- [2] W. Du, T. Wang, H.-S. Chu, C.A. Nijhuis, *Nature Photon.*, **11**, 623 (2017). DOI: 10.1038/s41566-017-0003-5
- [3] H.-S. Ee, Y.-S. No, J. Kim, H.-G. Park, M.-K. Seo, *Opt. Lett.*, **43**, 2889 (2018). DOI: 10.1364/OL.43.002889
- [4] Y. Fang, M. Sun, *Light: Sci. Appl.*, **4**, e294 (2015). DOI: 10.1038/lsa.2015.67
- [5] A. Liu, P. Wolf, J.A. Lott, D. Bimberg, *Photon. Res.*, **7**, 121 (2019). DOI: 10.1364/PRJ.7.000121
- [6] D. Liang, J.E. Bowers, *Nature Photon.*, **4**, 511 (2010). DOI: 10.1038/nphoton.2010.167
- [7] A.S. Polushkin, E.Y. Tiguntseva, A.P. Pushkarev, S.V. Makarov, *Nanophotonics*, **9**, 599 (2020). DOI: 10.1515/nanoph-2019-0443
- [8] J. Lambe, S.L. McCarthy, *Phys. Rev. Lett.*, **37**, 923 (1976). DOI: 10.1103/PhysRevLett.37.923
- [9] D.V. Lebedev, A.M. Mozharov, A.D. Bolshakov, V.A. Shkoldin, D.V. Permyakov, A.O. Golubok, A.K. Samusev, I.S. Mukhin, *Phys. Status Solidi (RRL)*, **14**, 1900607 (2020). DOI: 10.1002/pssr.201900607
- [10] S.W. Hla, *Rep. Prog. Phys.*, **77**, 056502 (2014). DOI: 10.1088/0034-4885/77/5/056502
- [11] S.W. Hla, *J. Vac. Sci. Technol.*, **23**, 1351 (2005). DOI: 10.1116/1.1990161
- [12] Z. Klusek, A. Busiakiewicz, P.K. Datta, R. Schmidt, W. Kozłowski, P. Kowalczyk, P. Dabrowski, W. Olejniczak, *Surf. Sci.*, **601**, 1513 (2007). DOI: 10.1016/j.susc.2007.01.011
- [13] V.M. Kornilov, A.N. Lachinov, *Microelectron. Eng.*, **69**, 399 (2003). DOI: 10.1016/S0167-9317(03)00327-7
- [14] S. Kondo, S. Heike, M. Lutwyche, Y. Wada, *J. Appl. Phys.*, **78**, 155 (1995). DOI: 10.1063/1.360733
- [15] S.V. Makarov, I.S. Sinev, V.A. Milichko, F.E. Komissarenko, D.A. Zuev, E.V. Ushakova, I.S. Mukhin, Y.F. Yu, A.I. Kuznetsov, P.A. Belov, I.V. Iorsh, A.N. Poddubny, A.K. Samusev, Yu.S. Kivshar, *Nano Lett.*, **18**, 535 (2018). DOI: 10.1021/acs.nanolett.7b04542
- [16] S.A. Kukushkin, A.V. Osipov, *Prog. Surf. Sci.*, **151**, 1 (1996). DOI: 10.1016/0079-6816(96)82931-5
- [17] V.G. Dubrovskii, *J. Chem. Phys.*, **131**, 164514 (2009). DOI: 10.1063/1.3254384
- [18] V.G. Dubrovskii, N.V. Nazarenko, *J. Chem. Phys.*, **132**, 114507 (2010). DOI: 10.1063/1.3354118
- [19] V.G. Dubrovskii, N.V. Sibirev, X. Zhang, R.A. Suris, *Cryst. Growth Des.*, **10**, 3949 (2010). DOI: 10.1021/cg100495b